Juvenile Pilocytic Astrocytomas: CT and MR Characteristics

Ya-Yen Lee, Pamela Van Tassel, Janet M. Bruner, Richard P. Moser and Jane C. Share

AJNR Am J Neuroradiol 1989, 10 (2) 363-370
http://www.ajnr.org/content/10/2/363

Juvenile Pilocytic Astrocytomas: CT and MR Characteristics

Ya-Yen Lee[1]
Pamela Van Tassel[1]
Janet M. Bruner[2]
Richard P. Moser[3]
Jane C. Share[4]

Thirty-seven cases of juvenile pilocytic astrocytoma were reviewed retrospectively to determine their CT and MR characteristics. All cases occurred in pediatric patients, except for one in a young adult. There was a propensity for tumors to be located around the third and fourth ventricles. On CT the tumors were all sharply demarcated and smoothly marginated and rarely had associated edema. The lesions tended to be round or oval. The tumor matrix was most often hypo- or isodense with marked enhancement. Cyst formation, either micro- or macrocystic or combined, was frequently observed, and tumor calcification occurred occasionally. On MR the tumors appeared hypo- or isointense on T1-weighted images and hyperintense on T2-weighted images.

The radiologic appearances of juvenile pilocytic astrocytomas are quite characteristic. By using age of presentation, typical location, configuration, and enhancement patterns, the presurgical diagnosis of juvenile pilocytic astrocytoma can be made with a high index of confidence.

Juvenile pilocytic astrocytoma is a distinctive histologic subtype of astrocytoma occurring predominantly in children and young adults and distinguished by a relatively benign clinical course. Histologically it has a characteristic appearance with an alternating pattern of compact bipolar pilocytic (hairlike) astrocytes and loosely aggregated protoplasmic astrocytes, the latter of which often undergo microcystic degeneration.

Although this astrocytoma is well known to neurooncologists and neurosurgeons, its radiologic characteristics have not been well described. In this retrospective study, we evaluated the CT and MR appearances of this distinctive astrocytoma in an attempt to improve presurgical diagnostic accuracy.

Materials and Methods

Thirty-seven cases of histologically proved juvenile pilocytic astrocytomas were collected for this retrospective study. The 17 males and 20 females were 6 months to 28 years old (mean, 7.1 years) at presentation. However, in 29 patients (78%) the disease was diagnosed within the first decade of life; there was only one adult (>20 years). Five patients (14%) had stigmata or a family history of neurofibromatosis.

Thirty-seven pretreatment CT and five MR studies were available for review. CT was performed routinely before and immediately after IV administration of iodinated contrast medium with a slice thickness of 4–10 mm; occasionally, delayed scans were obtained. T1-weighted spin-echo images, 600–800/17–20 (TR/TE); proton-density images, 2000/20–30; and T2-weighted images, 2000/80–90, were obtained in the MR studies. The location, size, configuration, and margins of the tumors were evaluated in addition to the CT density, contrast enhancement, and MR intensity. The presence of tumor calcification, micro- (diameter, ≤1 cm) or macro- (diameter, >1 cm) cyst formation, as well as associated edema or arachnoid cyst was also recorded.

Results

The locations of tumors were: optic chiasm and hypothalamus, 17; cerebellar vermis, seven; cerebellar hemisphere, four; cerebral hemisphere, four (three in the

This article appears in the March/April 1989 issue of *AJNR* and the June 1989 issue of *AJR*.

Received April 27, 1988; accepted after revision August 30, 1988.

[1] Division of Diagnostic Imaging, Department of Diagnostic Radiology, The University of Texas M. D. Anderson Cancer Center, 1515 Holcombe Blvd., Houston, TX 77030. Address reprint requests to Y.-Y. Lee.

[2] Division of Pathology, Section of Neuropathology, The University of Texas M. D. Anderson Cancer Center, Houston, TX 77030.

[3] Division of Surgery, Section of Neurosurgery, The University of Texas M. D. Anderson Cancer Center, Houston, TX 77030.

[4] Department of Radiology, Boston Children's Hospital, Boston, MA 02215.

***AJNR* 10:363–370, March/April 1989**
0195–6108/89/1002–0363

temporal lobe and one in the frontal lobe); intraventricular, two; septum pellucidum, one; thalamus, one; and optic nerve, one (Table 1). Among 17 cases of chiasmal lesions, nine had downward extension into the pituitary fossa (Fig. 1), three had anterior extension into the optic nerve (Fig. 2), and three had posterior extension into the postchiasmal optic pathway (Fig. 3). All four cerebellar hemispheric lesions were located medially near the vermis (Fig. 4). The two intraventricular tumors were identified within the anterior lateral ventricles (Fig. 5). The septal and thalamic lesions were located in the

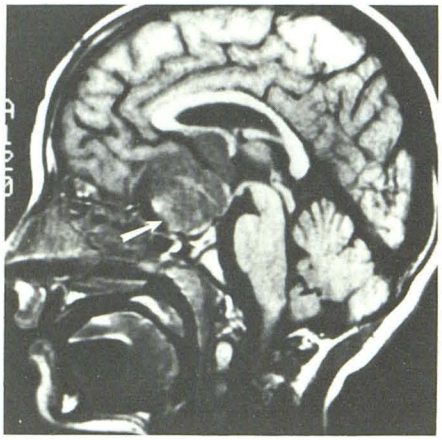

1

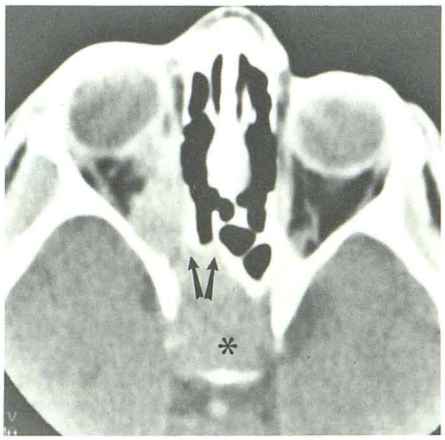

2

Fig. 1.—T1-weighted sagittal MR image, 600/20. Large chiasmal pilocytic astrocytoma with downward extension into pituitary fossa and sphenoid sinus (*arrow*).

Fig. 2.—Contrast-enhanced axial CT scan. Anterior extension of chiasmal pilocytic astrocytoma into right orbit. Noted are erosions of right tuberculum sellae and optic canal (*arrows*), as well as downward extension into pituitary fossa (*asterisk*).

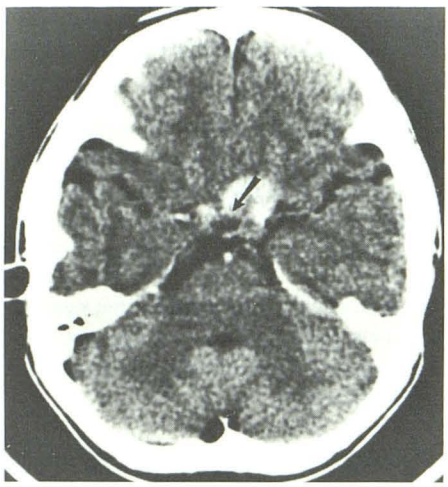

A

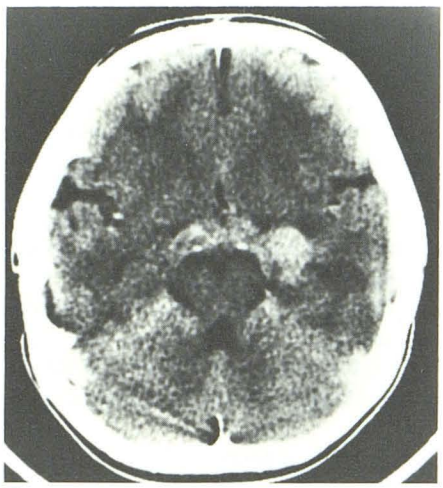

B

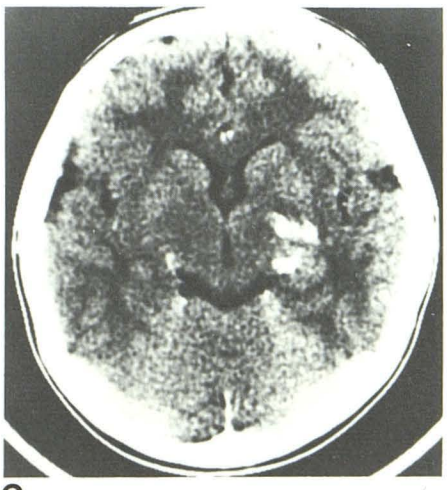

C

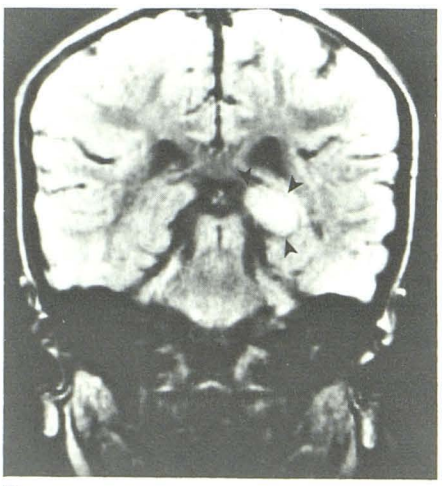

D

Fig. 3.—*A–C*, Contrast-enhanced axial CT scans show chiasmal pilocytic astrocytoma with bilateral postchiasmal optic pathway extension. Noted are tumor calcifications in left optic tract and microcyst in chiasmal tumor (*arrow*). Right optic tract is minimally involved, and there is uncertainty about left lateral geniculate body involvement.

***D*, Coronal proton-density MR image, 2000/20. Left lateral geniculate body involvement is definite and sharply delineated (*arrowheads*).**

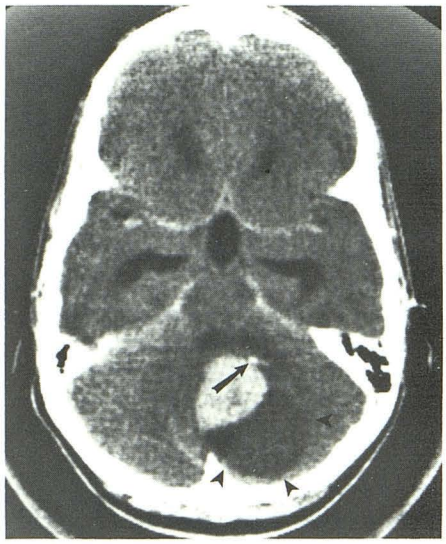

Fig. 4.—Contrast-enhanced axial CT scan shows cystic pilocytic astrocytoma of left medial cerebellar hemisphere. Noted are a small flecklike tumor calcification (*arrow*); a sharply demarcated, solid, enhancing component; and a macrocyst (*arrowheads*). Surrounding edema is minimal. Fourth ventricle is severely deformed with resultant obstructive hydrocephalus.

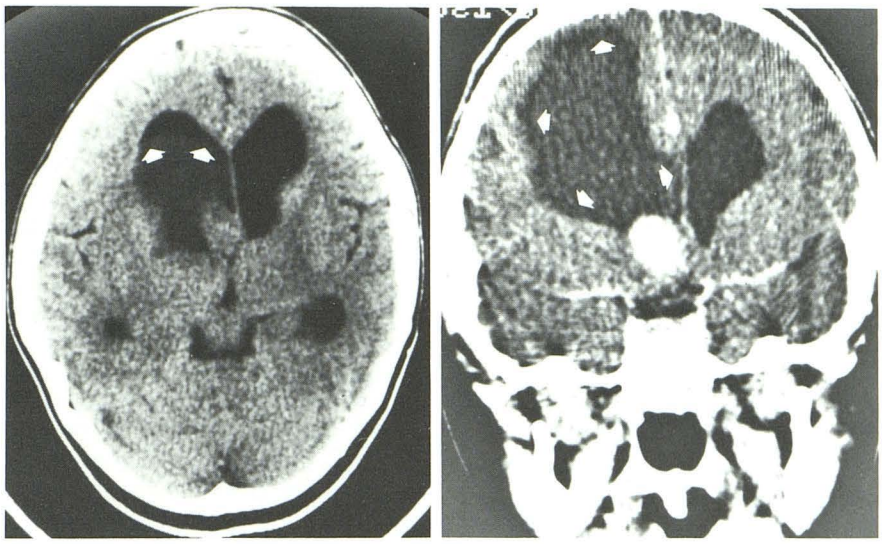

A B

Fig. 5.—Nonenhanced axial (*A*) and enhanced coronal (*B*) CT scans show intraventricular pilocytic astrocytoma. Large associated intraventricular cyst (*arrows*) has a CT attenuation number slightly higher than that of CSF.

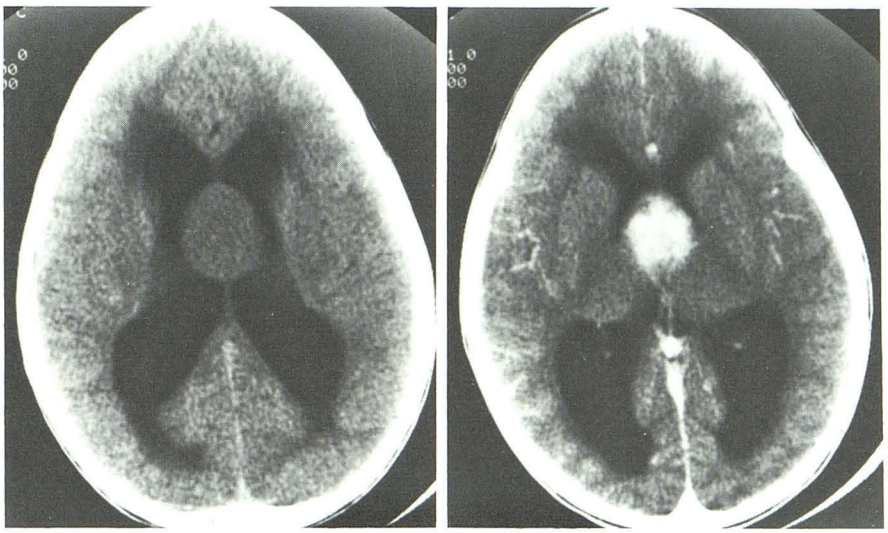

A B

Fig. 6.—Nonenhanced (*A*) and enhanced (*B*) axial CT scans show isodense enhancing pilocytic astrocytoma arising from septum pellucidum. This sharply demarcated round tumor was proved to be subependymal at surgery.

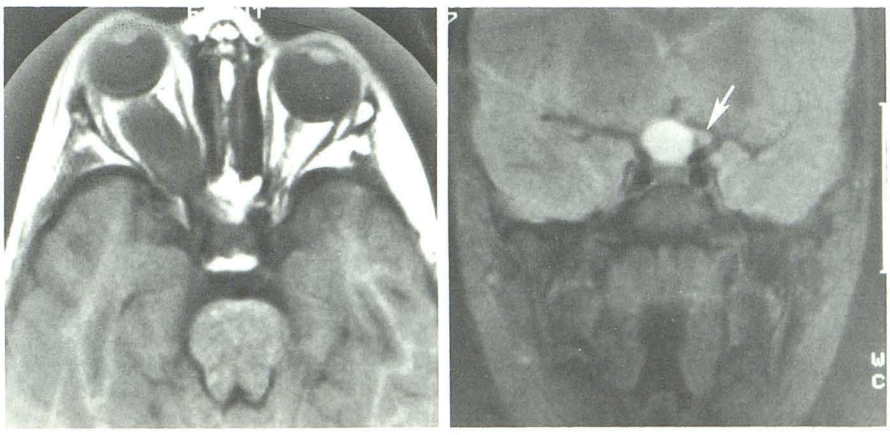

A B

Fig. 7.—T1-weighted axial, 600/17 (*A*), and T2-weighted coronal, 2000/90 (*B*), MR images show right optic nerve pilocytic astrocytoma with posterior extension into optic chiasm. Tumor is hypointense on T1- and hyperintense on T2-weighted images. Left side of optic chiasm is displaced but uninvolved (*arrow*).

TABLE 1: Summary of Juvenile Pilocytic Astrocytomas

Location	No.	Extension (No.)	Configuration (No.)	No. with Cyst Formation[a]	No. with Calcification	No. with Edema	CT Findings (No.)		MR Findings (No.)		No. with Associated Neurofibromatosis
							Tumor Matrix	Contrast Enhancement	T1	T2	
Optic chiasm/hypothalamus	17	Pituitary fossa (9), optic nerve (3), postchiasmal pathway (3)	Multilobulated (10), oval (4), dumbbell (3)	Micro (9), macro (1)	2	0	Hypodense (4), isodense (11), hyperdense (2)	Moderate (6), marked (11)	Hypointense (2), isointense (2)	Hyperintense (4)	3
Cerebellum:											
Vermis	7	No extension	Round (5), oval (2)	Micro (1), macro (3), combined (3)	0	0	Hypodense (2), isodense (5)	Marked (7)	MR not performed	*N*	0
Hemisphere	4	No extension	Round (3), oval (1)	Macro (3), combined (1)	1	1	Hypodense (2), isodense (2)	Moderate (1), marked (3)	MR not performed	*N*	0
Cerebrum:											
Hemisphere	4	No extension	Round (2), oval (2)	Macro (3)	0	1	Hypodense (3), isodense (1)	Marked (4)	MR not performed	*N*	0
Intraventricular	2	No extension	Oval (2)	Macro (1)	0	0	Hypodense (2)	Marked (2)	MR not performed	*N*	1
Subependymal	2	No extension	Oval (2)	No cysts	1	0	Hypodense (2)	Marked (2)	MR not performed	*N*	0
Optic nerve	1	Optic chiasm (1)	Dumbbell (1)	No cysts	0	0	Hypodense (1)	Marked (1)	Hypointense (1)	Hyperintense (1)	1

[a] Microcysts are ≤1 cm in diameter; macrocysts are >1 cm in diameter.

subependymal region around the third ventricle (Fig. 6). One lesion arose in an optic nerve with posterior extension into the optic chiasm (Fig. 7).

The majority of the tumors were either oval or round (23 cases, 62%). Ten lesions were multilobulated; all 10 were chiasmal. One optic nerve and three chiasmal lesions had a dumbbell appearance. The size of the tumors ranged from 2 × 2 × 2 cm^3 to 6 × 5 × 6 cm^3. All the lesions were sharply demarcated and smoothly marginated. The CT density of the tumor matrix was hypodense relative to brain in 16, isodense in 19, and hyperdense in two. All the tumors enhanced on CT after IV contrast administration, at least to a moderate degree and usually markedly. Tumor calcifications were identified in four cases (11%), including two chiasmal lesions, all in the form of flecks (Fig. 8). Twenty-five cases (68%) had cyst formation; microcysts were observed in 10 cases, macrocysts in 11 cases, and a combination of both in four (Fig. 9). Mild vasogenic edema was associated only in two cases, one in the cerebral and the other in the cerebellar hemisphere. An associated arachnoid cyst or subarachnoid-space dilatation was observed in two cases, one associated with a chiasmal lesion (Fig. 10) and the other one in the sylvian fissure with a temporal lesion. The tumors all appeared isointense or slightly hypointense relative to brain on T1-weighted and hyperintense on T2-weighted images in all five patients who had MR.

Discussion

Mature astrocytes are of fibrillary and protoplasmic types, both of which can give rise to astrocytomas. The diffuse astrocytomas of the cerebral hemispheres usually are of the fibrillary type (Fig. 11); this is because protoplasmic astrocytes can acquire fibrillary characteristics under pathologic conditions. Astrocytomas also may be categorized by histologic growth pattern. The pilocytic astrocytomas have an abundance of cells that are elongated and bipolar, thus appearing "hairlike." These tumors are of two distinct types: adult (or diffuse) and juvenile (or biphasic). The juvenile pilocytic astrocytoma has also been referred to as "polar spongioblastoma." Complicating the issue of pilocytic astrocytoma is the tendency of diffuse cerebral and pontine fibrillary astrocytomas of higher grades of anaplasia to infiltrate along existing brain fiber tracts, thus attaining an artificial pilocytic appearance (Fig. 12) [1].

The juvenile pilocytic astrocytoma is a distinct low-grade variant of astrocytoma, both clinically and histopathologically. It is composed of distinct areas of compact pilocytic astrocytes, mostly arranged around vessels, and mixed with areas having a looser, protoplasmic, or partially cystic appearance [2]. This gives a definite biphasic pattern to the tumor when viewed under low-power magnification (Fig. 13). In contrast to the diffuse fibrillary astrocytomas of the cerebral hemispheres, for which a grading system is well established [3], the presence of atypical or multinucleated cells or vascular endothelial hyperplasia does not imply a worse prognosis for the juvenile pilocytic neoplasms. Mitoses and tumor necrosis are found rarely or never [4]. Important histologic and CT features of various gliomas are outlined in Table 2.

Juvenile pilocytic astrocytomas may have a grossly cystic character and contain a mural tumor nodule located in the

Fig. 8.—Nonenhanced (*A*) and enhanced (*B*) axial CT scans show calcified chiasmal pilocytic astrocytoma. Noted are microcysts within this strongly enhancing tumor (*arrows*).

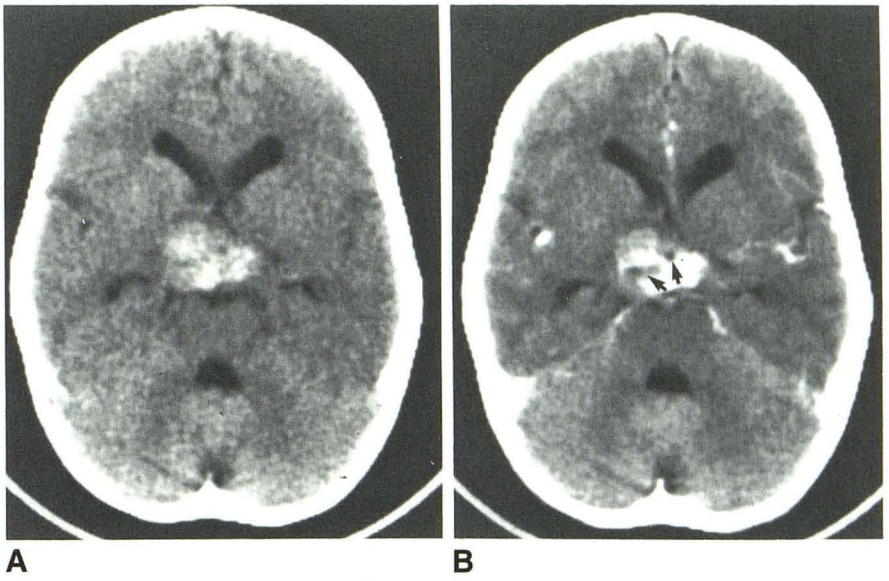

Fig. 9.—Contrast-enhanced axial CT scans.
A, Intraventricular pilocytic astrocytoma. Multiple microcysts are identified.
B, Right frontal pilocytic astrocytoma. Well-defined macrocyst is associated with strongly enhancing mural nodule.

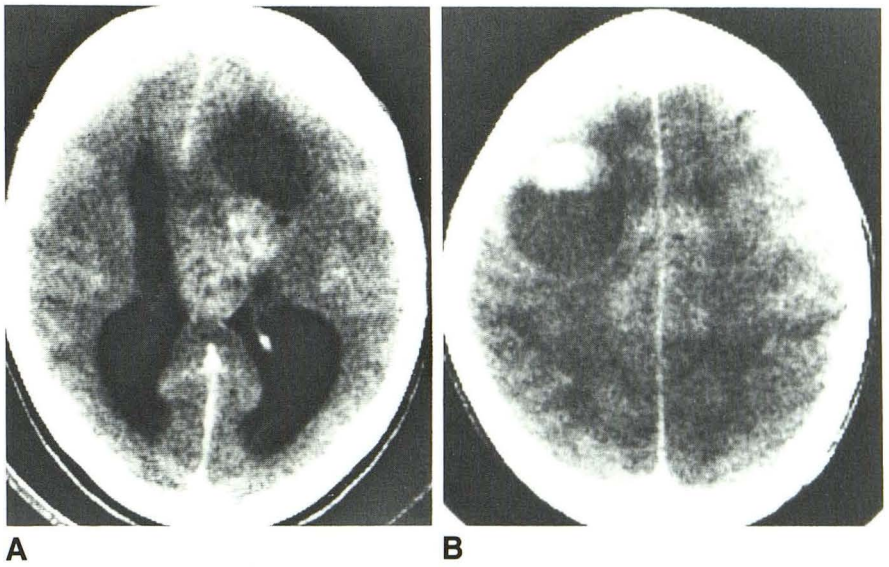

Fig. 10.—*A*, Contrast-enhanced axial CT scan shows strongly enhanced chiasmal pilocytic astrocytoma surrounded by multilobulated arachnoid cyst (*arrows*).
B, Coronal T2-weighted MR image, 2000/80, shows associated arachnoid cyst draped around tumor (*arrowheads*). Sagittal T1-weighted MR image, 600/20, in this patient (Fig. 1) did not provide demarcation of tumor from surrounding arachnoid cyst.

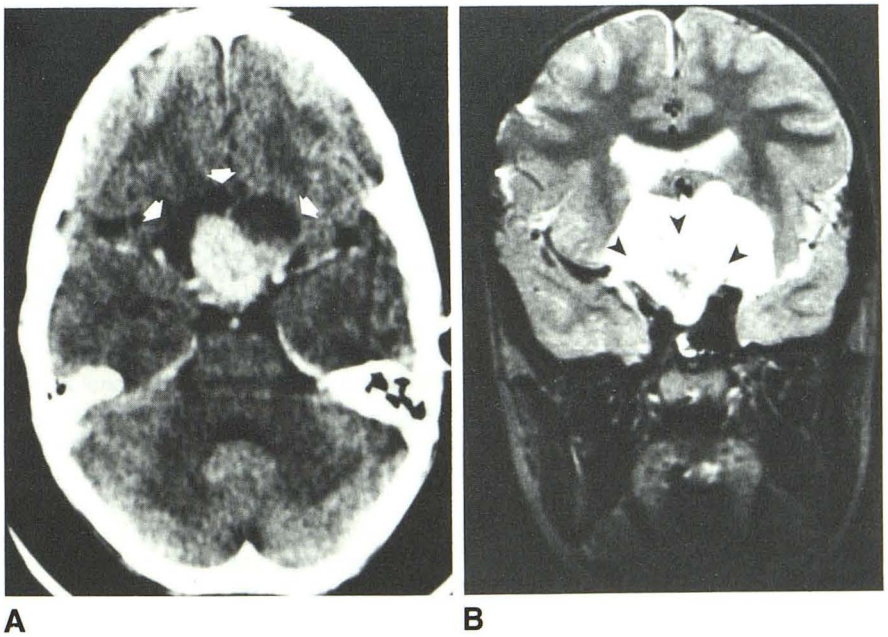

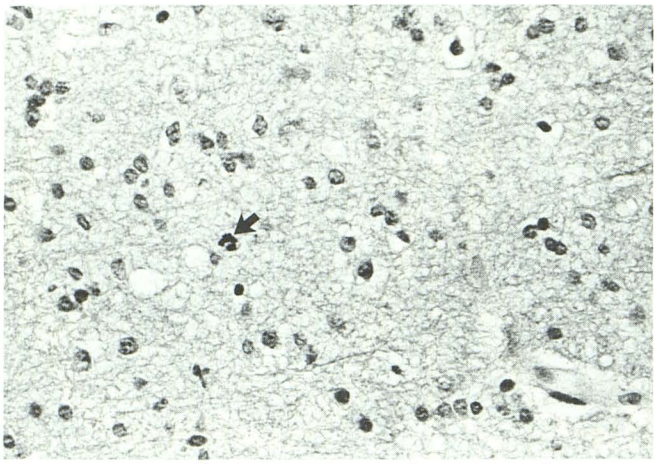

Fig. 11.—Diffuse fibrillary astrocytoma, low grade. Diagnostic features include uneven increase in cellularity, nuclear enlargement, and rounded nuclei with multiple delicate fibrillary processes. One mitotic figure (*arrow*) is present. (H and E, ×600)

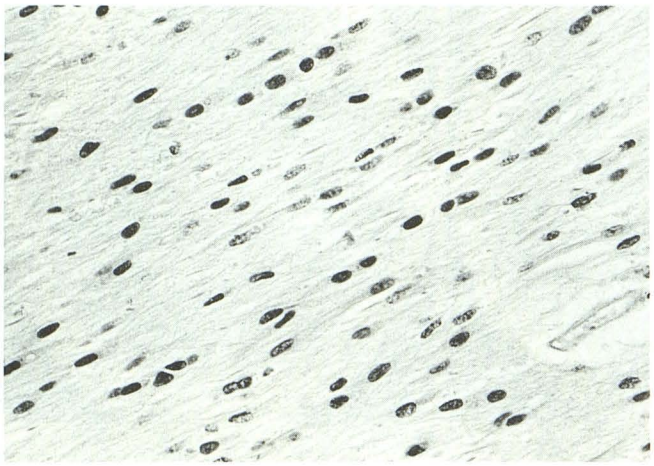

Fig. 12.—Pilocytic growth pattern in pontine glioblastoma multiforme. Neoplastic cells are elongated, with bipolar processes, but growth pattern is diffuse. Other areas of this neoplasm were highly pleomorphic and showed coagulation necrosis. (H and E, ×600)

wall of the cyst. This tumor nodule is soft and red-tan, because of rich vascularity. The tumors commonly occur in children and young adults. The most frequent locations are the cerebellum, the optic nerves or chiasm (optic-nerve glioma), and the region around the third ventricle. Less often, juvenile pilocytic astrocytomas can be found in the cerebral hemispheres and lateral ventricles. These tumors are the most common astrocytic neoplasm in the cerebellum of children. The diffuse (adult type, nonbiphasic) pilocytic astrocytomas are distinctly less common than the juvenile type in children. Biologically, the juvenile tumors are low grade. After complete surgical excision, they almost never recur. Even those examples that are incompletely resected are slow growing, and, unlike diffuse astrocytomas of the cerebrum, do not undergo malignant transformation to a more anaplastic form [4].

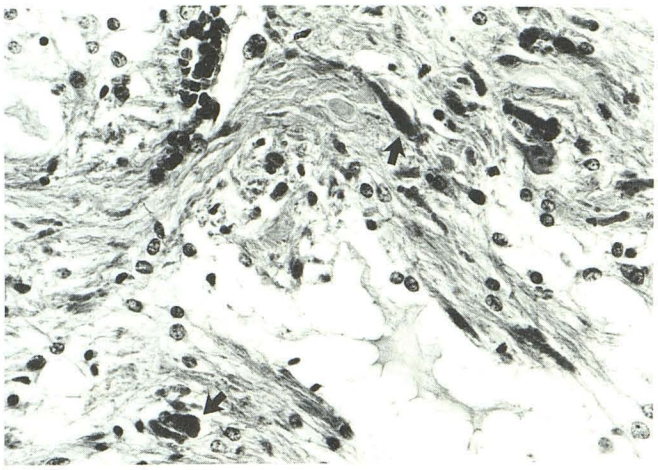

Fig. 13.—Juvenile pilocytic astrocytoma. Characteristic biphasic pattern of dense "hairlike" pilocytic areas alternating with looser microcystic areas. Rosenthal fibers can be identified (*arrows*). (H and E, ×600)

Juvenile pilocytic astrocytomas are well known for their association with neurofibromatosis, and in this entity they are usually confined to the anterior optic pathways; for example, the optic nerve and chiasm [5–8]. In our series five juvenile pilocytic astrocytomas were associated with neurofibromatosis; three were centered at the optic chiasm, one involved the optic nerve, and one was within the frontal horn of the lateral ventricle.

Several characteristic findings were observed in our radiologic review. Except for occasional hemispheric lesions, these tumors tend to be found around the third ventricle supratentorially and the fourth ventricle infratentorially; that is, in the optic chiasm and vermis, respectively. All lesions appear sharply demarcated and smoothly marginated and often are round or oval in configuration, except when located in the optic chiasm or optic nerve. At these sites the tumor has a tendency to grow along the optic pathway, giving a multilobulated or dumbbell appearance. Most often the tumor matrix appears hypo- or isodense and enhances strongly on CT. The character of contrast enhancement of juvenile pilocytic astrocytomas is distinctive when compared with the more frequently occurring low-grade fibrillary astrocytomas, which often present as hypodense, nonenhancing masses [9, 10]. This CT observation might be explained by increased tumor vascularity, which is constantly observed in the pilocytic astrocytomas and absent in the low-grade fibrillary astrocytomas. The frequent absence of associated edema is indicative of the low malignancy of this particular astrocytoma. Interestingly, two patients in our series were seen initially with an arachnoid cyst draped around the tumor. Its indolent growth and tendency to infiltrate along the arachnoid with secondary fibrotic changes might explain the secondary development of an arachnoid cyst. To our knowledge, this has not been reported in association with other brain tumors. Tumor calcification, which occurred rarely, tends to be flecklike. Formation of either micro- or macrocysts is observed frequently in pilocytic astrocytomas. Macrocysts tend to occur in cerebral or cerebellar lesions and rarely in the lesions along the optic

TABLE 2: Histologic and CT Features of Various Gliomas

Type of Glioma	Histology	CT
Pilocytic astrocytoma (polar spongioblastoma)	Bipolar and biphasic; increased vascularity; mitosis and necrosis rare or never	Around or in the ventricles; round or oval, multilobulated in chiasmal region; sharply demarcated; contrast enhancement marked; cysts frequent; calcification rare
Fibrillary astrocytoma: (Low-grade) astrocytoma	Multipolar fibrillary or protoplasmic; no increased vascularity	Lobar; round; poorly demarcated; hypodense, nonenhancing; cysts rare; calcification rare; edema?
Anaplastic astrocytoma	Multipolar fibrillary or protoplasmic; mitosis and vascular endothelial proliferation; no necrosis	Lobar; configuration variable; demarcation variable; contrast enhancement variable; cysts rare; calcification rare; edema frequent
Glioblastoma multiforme	Multipolar; markedly cellular and pleomorphic; mitosis and vascular endothelial; proliferation marked; necrosis required	Lobar; multilobulated; necrotic center frequent; cysts rare; calcification rare; edema frequent
Oligodendroglioma	Neoplastic oligodendrocytes with round nuclei and clear cytoplasm; prominent fine capillary branching	Peripheral lobar, occasionally around or in ventricle; demarcation variable; contrast enhancement variable; cysts occasional; calcification frequent; edema variable

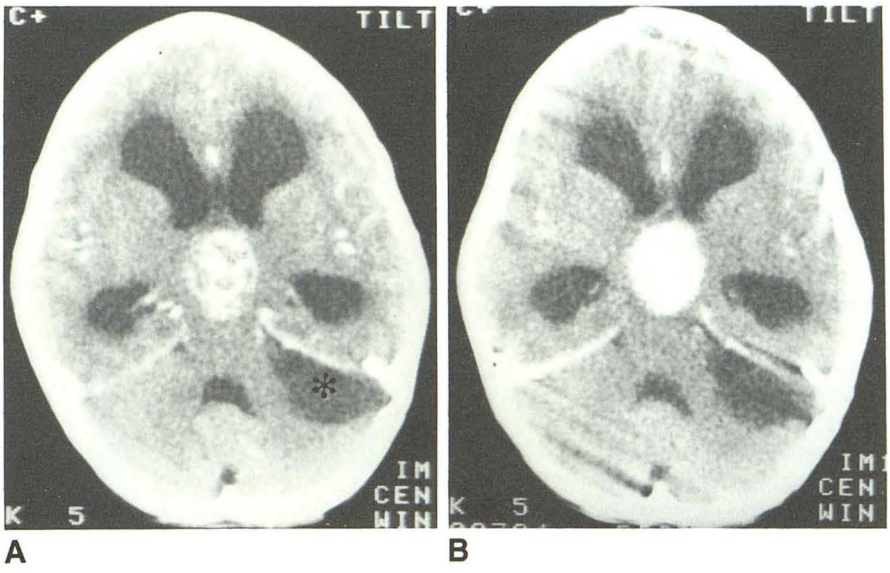

Fig. 14.—*A*, Immediate contrast-enhanced CT scan shows multiple microcysts within chiasmal pilocytic astrocytoma. Also noted is arachnoid cyst (*asterisk*).

***B*, Delayed contrast-enhanced CT scan. Microcysts fill with contrast medium.**

pathway or around the third ventricle. The microcysts are best demonstrated on the immediate postcontrast CT scans because these cysts may fill with contrast medium on delayed scans (Fig. 14). Comparison between MR and concurrent CT scans shows MR to be superior in delineating the tumor extent, particularly in the postchiasmal optic pathway [8, 11, 12].

The differential diagnosis of juvenile pilocytic astrocytoma includes craniopharyngioma, germinoma, loculated leptomeningeal metastasis, and invasive pituitary adenoma in the chiasmal region; medulloblastoma and ependymoma in the posterior fossa; and intraventricular or subependymal oligodendroglioma and ependymoma in the paraventricular cerebral hemisphere. Craniopharyngiomas tend to be densely calcified and often have macrocysts [13], while chiasmal pilocytic astrocytomas calcify rarely and the cysts are often

small and multiple. Suprasellar germinoma [14] and loculated leptomeningeal metastasis, most often from medulloblastoma in children, can mimic chiasmal pilocytic astrocytoma but without extension into the optic apparatus. These other tumors are often associated with evidence of diffuse leptomeningeal metastases, a finding never observed in pilocytic astrocytoma. Chiasmal pilocytic astrocytomas remain centered in the suprasellar region when they extend into the pituitary fossa, while this midline growth may not be observed when invasive pituitary adenomas extend into the suprasellar cistern. Furthermore, the compressed but noninfiltrated optic chiasm in pituitary adenomas can be appreciated readily on state-of-the-art imaging such as MR. Within the posterior fossa, in contrast to medulloblastoma and ependymoma, which tend to fill and dilate the fourth ventricle, the cerebellar pilocytic astrocytoma often extrinsically obliterates the ventricle. Macrocysts, often observed in cerebellar pilocytic astrocytomas, rarely occur in the former two tumors. Oligodendroglioma within or around the third or lateral ventricles [15, 16] may be very difficult to distinguish from a paraventricular pilocytic astrocytoma, but the age of the patient may provide an important differentiating clue.

In conclusion, the radiologic appearance of pilocytic astrocytomas is quite characteristic although not pathognomonic. They tend to be round or oval, sharply demarcated with smooth margins, usually without vasogenic edema, and located around the third or fourth ventricle. The tumor matrix is often hypo- or isodense on CT with strong contrast enhancement and frequent demonstration of micro- or macrocysts. On the basis of the typical radiologic appearance and age of the patient, a presurgical diagnosis of juvenile pilocytic astrocytoma can be made with confidence.

REFERENCES

1. Russell DS, Rubinstein LJ. *Pathology of tumors of the nervous system*, 4th ed. Baltimore: Williams & Wilkins, **1977**:156–163
2. Garcia DM, Fulling KH. Juvenile pilocytic astrocytoma of the cerebrum in adults. *J Neurosurg* **1985**;63:382–386
3. Burger PC, Vogel FS, Green SB, Strike TA. Glioblastoma multiforme and anaplastic astrocytoma: pathologic criteria and prognostic implications. *Cancer* **1985**;56:1106–1111
4. Clark GB, Henry JM, McKeever PE. Cerebral pilocytic astrocytoma. *Cancer* **1985**;56:1128–1133
5. Blah J, Jaffe R, Deutsch M, Adkins JC. Neurofibromatosis and childhood tumors. *Cancer* **1986**;57:1225–1229
6. Jacoby CG, Go RT, Beren RA. Cranial CT of neurofibromatosis. *AJNR* **1980**;1:311–315
7. Alvord EC, Lofton S. Gliomas of the optic nerve or chiasm. *J Neurosurg* **1988**;68:85–98
8. Brown EW, Riccardi VM, Mawad M, Handel S, Goldman A, Bryan RN. MR imaging of optic pathways in patients with neurofibromatosis. *AJNR* **1987**;8:1031–1036
9. Steinhoff H, Lanksch W, Kazner E, et al. Computed tomography in the diagnosis and differential diagnosis of glioblastomas. *Neuroradiology* **1977**;14:193–200
10. Marks JE, Gado M. Serial computed tomography of primary brain tumors following surgery, irradiation, and chemotherapy. *Radiology* **1977**; 125:119–125
11. Albert A, Lee BCP, Saint-Louis L, Deck MDF. MRI of optic chiasm and optic pathways. *AJNR* **1986**;7:255–258
12. Daniels DL, Herfkins R, Gager WE, et al. Magnetic resonance imaging of the optic nerve and chiasm. *Radiology* **1984**;152:79–83
13. Fitz CR, Wortzman G, Harwood-Nash DC, Holgate RC, Barry J, Boldt DW. Computed tomography in craniopharyngiomas. *Radiology* **1987**;127: 687–691
14. Fields JN, Fulling KH, Thomas PRM, Marks JE. Suprasellar geminoma: radiation therapy. *Radiology* **1987**;164:247–249
15. Dolinskas CA, Simeone FA. CT characteristics of intraventricular oligodendrogliomas. *AJNR* **1987**;8:1077–1082
16. Lee YY, Van Tassel P. Intracranial oligodendrogliomas: imaging findings in 35 untreated cases. *AJNR* **1989**;10:119–127